Nonlinear Vibrations of Structures Induced by Dry Friction

PETER STELTER

University of Hannover, Institute of Mechanics, Appelstrasse 11, D-3000 Hannover 1, Germany

(Received: 14 June 1990; accepted: 27 January 1992)

Abstract. The chattering of machine tools, the squealing noise generated by tram wheels in narrow curves and the noise of band saws are examples of physical processes in which elastic structures exhibit self-sustained stick-slip vibrations. The nonlinear contact forces are often due to dry friction. Periodic, multiperiodic, and chaotic motions can occur, depending on the parameters.

Because the governing equations of motion are non-integrable, solutions can only be determined by numerical integration methods. The numerical investigations of continuous structures requires the *modal approach* to reduce the number of degrees of freedom.

As an example, a beam system has been investigated numerically and experimentally in this paper. The nonlinear motion of a point of the continuous structure has been measured by a specially developed *laser vibrometer*.

The friction characteristic has been measured directly and identified from a measured time series by means of a *modal state observer*. The correlation dimension, which represents a lower bound of the *fractal dimension*, has been calculated using the *correlation integral* method from a measured time series of the beam system.

Key words: Stick-slip vibrations, laser vibrometer, modal state observer, correlation dimension.

1. Introduction

Over the last few decades many publications have appeared on the subject of nonlinear dynamics. Engineering problems in which chaotic motions were found by numerical integration and/or by experiment have been described by several authors. Moon and Shaw [1] analyzed a vibrating beam with nonlinear boundary conditions. Hendriks [2] and Springer and Ullrich [3] investigated the motion of a needle in a matrix printer. Szczygielski [4] considered the motion of a rotor touching a wall. Kaas-Petersen and True [5] treated the lateral motion of a railway bogie. Grabec [6] introduced a model for the chaotic chattering of a machine-tool. Pfeiffer [7] revealed chaotic motions in rattling gear drives.

An important problem in the field of mechanical engineering is dry or Coulomb friction, because it appears in two different phenomena in nature:

- As a resistance against the beginning of a motion from equilibrium (stick mode). The friction force is thus a *constraining* force.
- As a resistance against an existing motion (slip mode), in which the friction force is an *applied* force.

In an oscillatory motion both phenomena take place successively, resulting in a *stick-slip motion*. When dry friction is modeled in terms of a friction characteristic, where the kinetic friction coefficient is smaller than the static coefficient, *self-sustained* oscillations may also occur, cf. Magnus [8], Marui and Kato [9], Miyamoto [10] and Den Hartog [11]. During the stick mode

Nonlinear Dynamics **3**: 329–345, 1992.

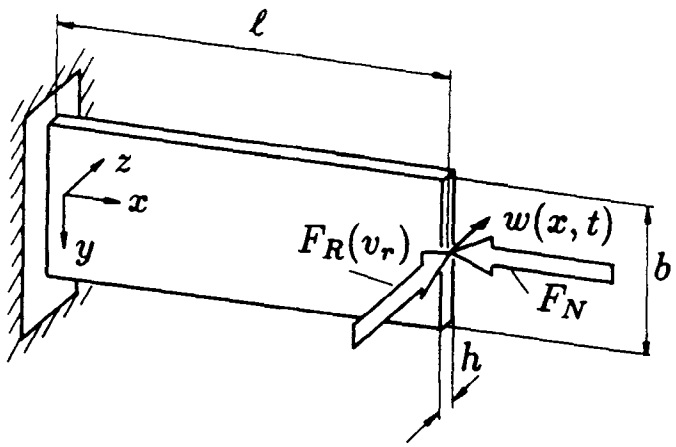

Fig. 1. Cantilever excited by a dry friction force.

some degrees of freedom are constrained, and hence these systems assume the character of a *variable structure*, where the number of state coordinates changes with time, cf. [7], [12]. In the case of dry friction the transition between the different modes is not *smooth* and is separated by a surface in the state space, cf. Utkin [13]. Due to the non-smooth character of the equations, chaotic motions can occur, as well as periodic and multiperiodic solutions. Some other papers addressing the dry friction problem have been published by Pratt and Williams [14], Dowell and Schwartz [15], Ferri and Dowell [16] and Shaw [17].

The aim of our research was to study *continuous* structures under the excitation of dry friction forces. Numerical investigations with a plate and a beam have shown that, due to the non-smooth equations of motion, the investigation of the long-term behaviour needs large amounts of CPU time. Therefore the first task was to develop effective numerical, analytical and experimental tools to handle these complex systems.

In order to study the behaviour of self-sustained vibrations induced by dry friction, the beam system shown in Figure 1 has been investigated both numerically and experimentally. From this simple system one can learn how continuous structures behave under the action of dry friction forces. The aim is to develop a mathematical model for this system and to verify the model assumptions by means of an experiment. In the case of an experimentally obtained irregular motion it is necessary to determine the *fractal dimension* of the chaotic attractor, in order to obtain a hint about the dimension of an appropriate mathematical model.

2. Numerical Investigation of the Beam System

The vibrating parts in engineering systems are usually *continuous* structures. If the deformations are small and the material behaves elastically, the continuous part of the structure can be treated as a *linear* system. The nonlinear friction force F_R acts at the tip of the beam system, as shown in Figure 1. The system is governed by the partial differential equation (PDE), equation (1)

$$w_{,\xi\xi\xi\xi} + \frac{l^2 F_N}{EI}\left[w_{,\xi\xi} - \delta(\xi - 1) w_{,\xi}\right] + \frac{l^4 \rho A}{EI} w_{,tt} = \frac{l^3 F_R(v_r)}{EI}\delta(\xi - 1)\,. \tag{1}$$

Where $\xi := x/l$ denotes the dimensional length coordinate of the beam, F_N is the normal force, EI is the bending stiffness, ρ is the density, A the cross-section, $(*)'$ denotes the partial derivative with respect to time or space, and $v_r = w_{,t}(\xi = 1) - v_0$ is the relative velocity, where v_0 is a constant belt velocity. The δ-distribution allows us to take account of the discrete forces. In the following sections, the normal force F_N has been neglected, because experiments show that its influence is small.

Equation (1) can be reduced to a set of first-order systems of ordinary differential equations (ODEs) by the modal approach

$$w(\xi, t) = \sum_{i=1}^{m} \phi_i(\xi) q_i(t) . \tag{2}$$

With the modal coordinates q_i, which are arranged in the state vector $\boldsymbol{x}^T = [q_1, q_1', q_2, q_2', \ldots, q_{2n}, q_{2n}']$ the equation of motion read in nondimensional state space notation is

$$\left.\begin{aligned} x_{2j-1}' &= x_{2j} , \\ x_{2j}' &= -2D_j\lambda_j x_{2j} - \lambda_j^2 x_{2j-1} + \lambda_j^2 \frac{F_R(v_r)}{F_{RS}} , \end{aligned}\right\} , j = 1(1)n , \tag{3}$$

with x_j being the state variables, D_j the modal damping factors, $\lambda_j = \omega_j/\omega_n$ the scaling factors, and n the number of state variables. The friction force

$$F_R(v_r) = -\tilde{\mu}(v_r) F_N \operatorname{sgn}(v_r) \tag{4}$$

is scaled by the friction force $F_{RS} = F_R(v_r = -v_0)$ at the *equilibrium position*. In vector notation, equation (3) has the following structure

$$\boldsymbol{x}' = \boldsymbol{A}\boldsymbol{x} + \boldsymbol{r}(\boldsymbol{x}) , \tag{5}$$

with the linear system matrix $\boldsymbol{A}$, and the vector $\boldsymbol{r}(\boldsymbol{x})$ of the friction forces, which depends nonlinearly on the state vector $\boldsymbol{x}$.

The functions ϕ_i can be chosen as any set of orthogonal functions. Here, the first two (real) eigenfunctions of the bending motion, equation (6), have been taken into account.

$$\tilde{\phi}(\xi) = \frac{\cos(k_i) + \cosh(k_i)}{\sin(k_i) + \sinh(k_i)} [\sin(k_i\xi) - \sinh(k_i\xi)] - [\cos(k_i\xi) - \cosh(k_i\xi)] . \tag{6}$$

These are shown in Figure 2. The eigenvalues are $k_1 = 1.875$ and $k_2 = 4.694$. The eigenfunctions of the beam system have also been measured, and the modal parameters have been fitted through a *modal analysis*. Furthermore, the modal damping factors D_j can only be determined by this method. The damping factors are $D_1 = 0.00015$ and $D_2 = 0.00085$. A more detailed report addressing this problem is given in [20] and [21].

A typical question in engineering practice is: how many mode shapes have to be taken into account in order to obtain sufficient accuracy. In the context of linear systems, this question can be answered by frequency domain analysis. As we will see in Section 3, this method is not practicable in the case of nonlinear systems, because a nonlinear system does not necessarily vibrate at frequencies close to its *natural* frequencies. In order to determine how many mode

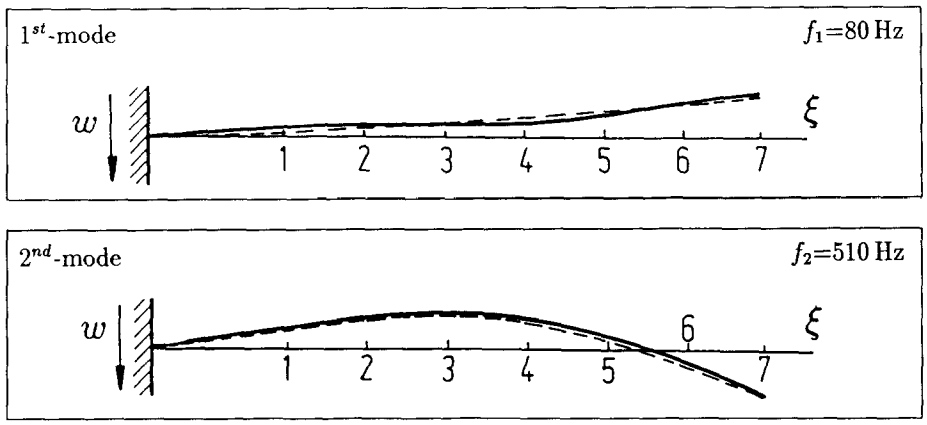

Fig. 2. The first two bending modes shapes of the unloaded ($F_N = 0$) beam system (—— measured, – – – calculated).

shapes have to be taken into account in the numerical studies, the limit cycle has been calculated, for different numbers of mode shapes. The results can be seen in Figure 3. With only one mode shape the system behaves like a system with a single degree of freedom. As the number of mode shapes increases, the limit cycle converges to its characteristic shape. In order to save CPU time, only *two* mode shapes have been used in the following numerical investigations.

Another task which has to be addressed is the determination of the friction force between the steel cantilever and the polyurethane belt. The friction characteristic $\tilde{\mu}$ has therefore been measured with a specially developed device, see Figure 4. The results of the measurements are also given in Figure 4. The broad band of fluctuation in the measurements is caused by the change of the friction coefficient along the length of the belt and by the dynamics of the measuring device itself, cf. [19]. An alternative way to determine the friction characteristic will be explained in Section 5.

The measured mean values have been approximated by an exponential law, equation (7)

$$\tilde{\mu}(v_r) = 0.66\left[0.5 + 0.5\exp\left(\frac{c_1}{|v_r|}\right)\right]\left[0.5 + 0.5\exp(c_2|v_r|)\right], \tag{7}$$

with the constants $c_1 = -0.02\,\mathrm{m/s}$ and $c_2 = -0.25\,\mathrm{s/m}$. This friction law has been used for the numerical studies.

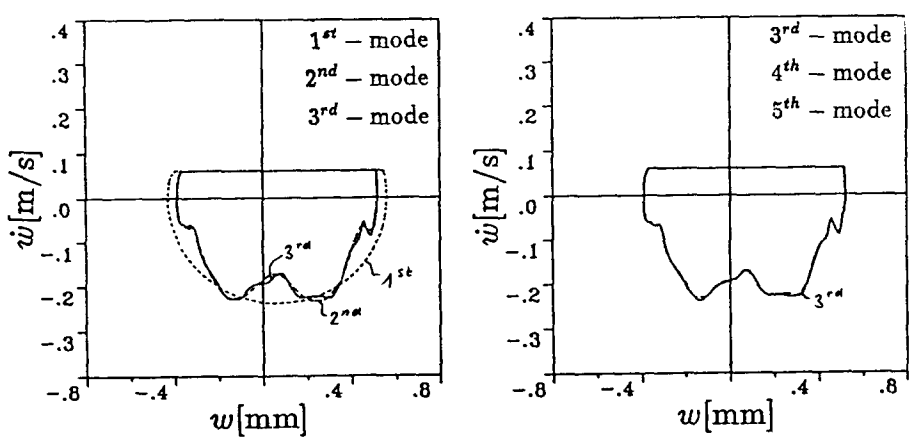

Fig. 3. Nonlinear limit cycles of the beam system at different numbers of mode shapes.

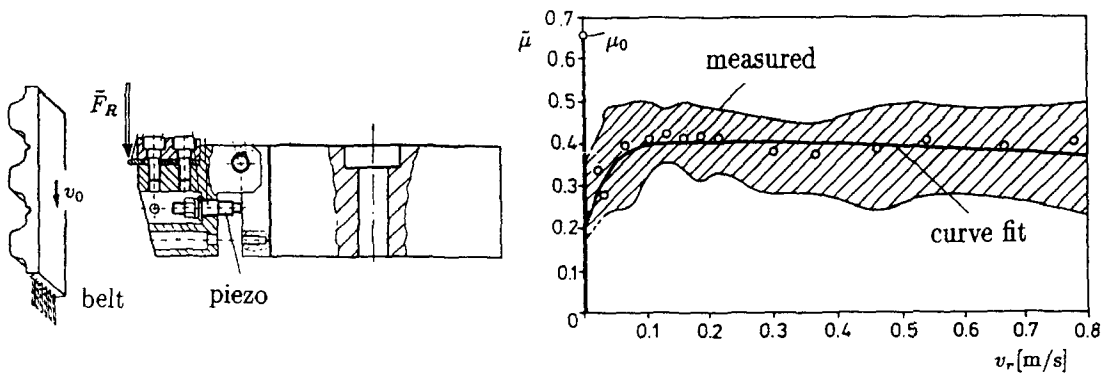

Fig. 4. Measurement device for the friction force and measured friction characteristic $\tilde{\mu} := \tilde{F}_R/\tilde{F}_N$ ($\circ$ = mean values).

3. Bifurcation Behaviour of the Beam System

In order to obtain an overview of the system's behaviour, the bifurcations with respect to the normal force F_N and the belt velocity v_0 have been investigated numerically. To reveal the overall response of the beam system it is sufficient to examine the motion of the continuous structure at one point, because the amplitudes at other positions are only *weighted* by the mode shapes.

The control, or bifurcation parameter, F_N, has been plotted in Figure 5 against the amplitude w_P, at vanishing velocity, $w_P := w(x = l) \wedge \dot{w}(x = l) = 0$. This point can be understand as a Poincaré section at $\dot{w} = 0$. The transition from the sticking mode to the slipping mode occurs when the friction force equals the restoring force. This is only valid under *static* conditions. The transition amplitude w_A can be calculated from equation (8).

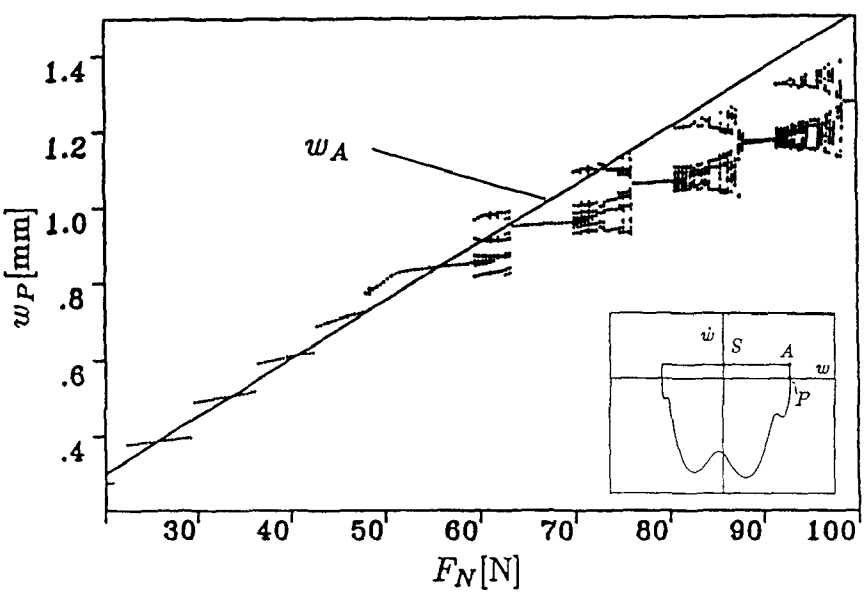

Fig. 5. Numerically generated bifurcation diagram for the normal force with a belt velocity of $v_0 = 60$ mm/s.

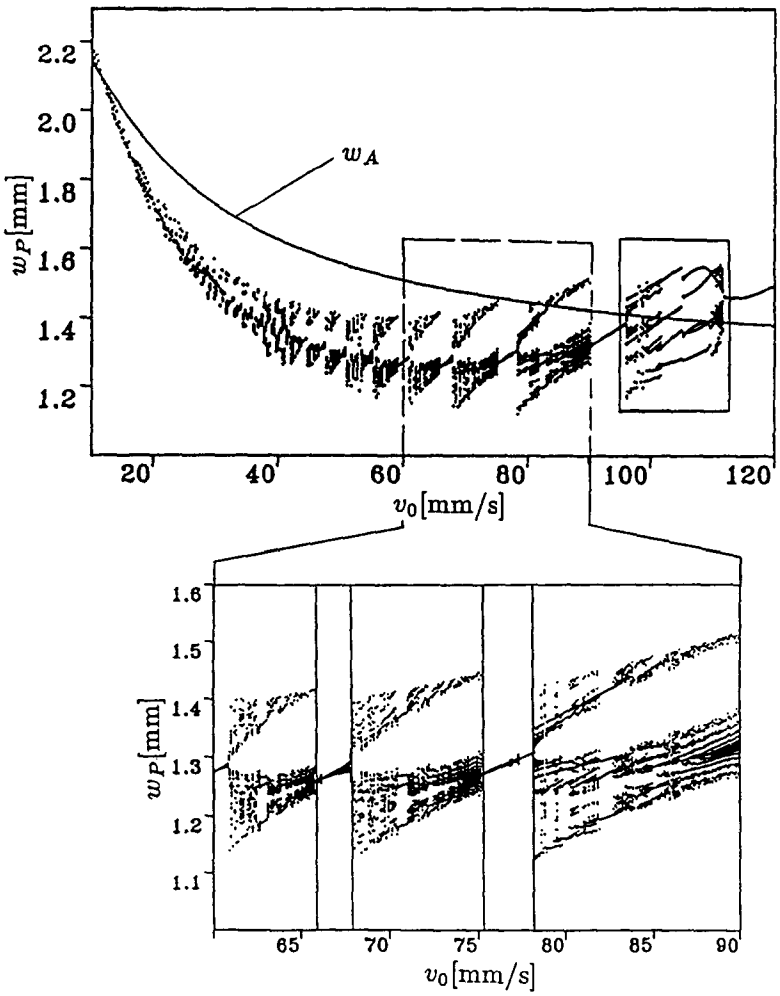

Fig. 6. Numerically generated bifurcation diagram for the belt velocity with a normal force of $F_N = 100$ N.

$$w_A(F_N, v_0) = \frac{F_N l^3}{3EI} (\mu_0 - \tilde{\mu}(v_0)) . \tag{8}$$

The reader can easily see that the amplitude w_A depends linearly on the normal force. More complicated motions can occur in the dynamic case, as shown in Figure 5. Period-one solutions are interrupted by multiperiodic solutions. The bifurcation scheme does not fit the usual bifurcation scenarios, such as period doubling cascades or intermittancy.

Figure 6 shows the bifurcation behaviour with respect to the belt velocity. The static amplitude w_A depends on the friction characteristic, referring to equation (8). A magnification of the domain from $v_0 = (60 \ldots 90)$ mm/s shows the strange bifurcation behaviour. As seen in Figure 7, a magnification of the region of $v_0 = (96 \ldots 112)$ mm/s shows period-one, period-four, and irregular-looking motions, as well as other multiperiodic motions. If we wish to make further statements about the bifurcation behaviour we need to take account of sophisticated tools, like *bifurcation theory*. This has been done for a two-mass system in [22].

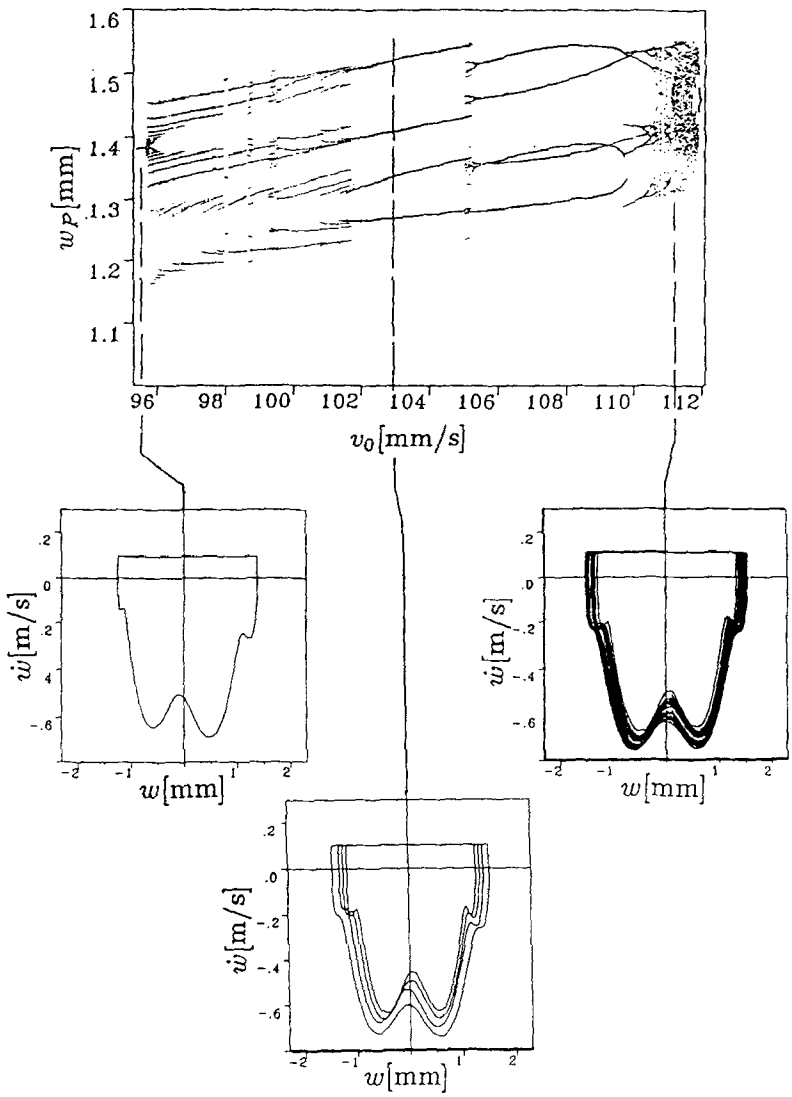

Fig. 7. Magnification with a period-one, a period-four, and an irregular motion.

4. Comparison with Experimental Data

The ODEs (3) have been solved with the program language ACSL and a Runge–Kutta–Fehlberg scheme of the fifth order. In order to verify the model assumptions, measurements have been carried out with an experimental test set-up, cf. Figure 8. The motion of the tip of the cantilever has been measured by a specially developed *laser interferometer*. This non-contact measurement device allows one to observe the deflection of the tip with a high precision. This turned to be out necessary, in order to reveal the nonlinear character of the motion of the beam system, e.g. the 'flat top' of the phase plots. Figure 9 shows the phase plots of the tip of the beam, *measured* by the

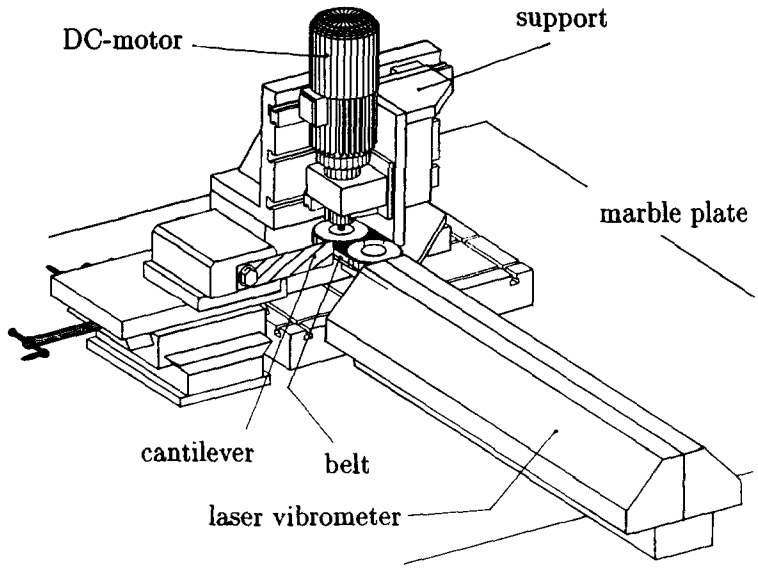

Fig. 8. Test set-up with the beam system and the laser vibrometer.

laser vibrometer. From the plots the reader can see that an increasing belt velocity leads to more 'harmonic' motions, and that an increase of the normal force leads to longer sticking regions and higher harmonics show up: see also the Fourier spectra in Figure 10. This diagram also shows that the main limit cycle frequency is about 40 Hz, but the first two natural frequencies are at 80 Hz and 510 Hz, which means that the natural frequencies do not show up in the Fourier spectra for the nonlinear system. This means that, due to the friction forces, the motion takes place at a lower frequency than the *first* natural bending frequency. But the characteristic shape of the limit of cycle also requires the *second* bending model to be taken into account.

Figure 11 shows a comparison of the measured and simulated phase plots and amplitude spectrum of the cantilever at different belt velocities. The phase-plane plots show that the tip of the cantilever vibrates in a stable limit cycle. Many simulations and measurements show that the results coincides within a wide parameter range. Figure 12 shows part of the v_0, F_N parameter space. The areas with period-one solution are marked by dashed boundaries. No self-sustained vibrations take place in the hatched regions. The measured data points have the same behaviour are marked by dots in this figure.

The experimental investigations showed that the dry friction dominated the resulting motion. Due to the unavoidable fluctuation of the friction force no stable two- or four-periodic solutions have been obtained, as in the numerical investigations. At some parameter combinations of v_0 and F_N irregular motions have also been measured. The question of how these complex types of motion can be handled will be addressed in Section 6.

It should be mentioned that the fluctuation of the friction forces has not been modelled in the analysis; otherwise a mixing between stochastic and deterministic forces will occur.

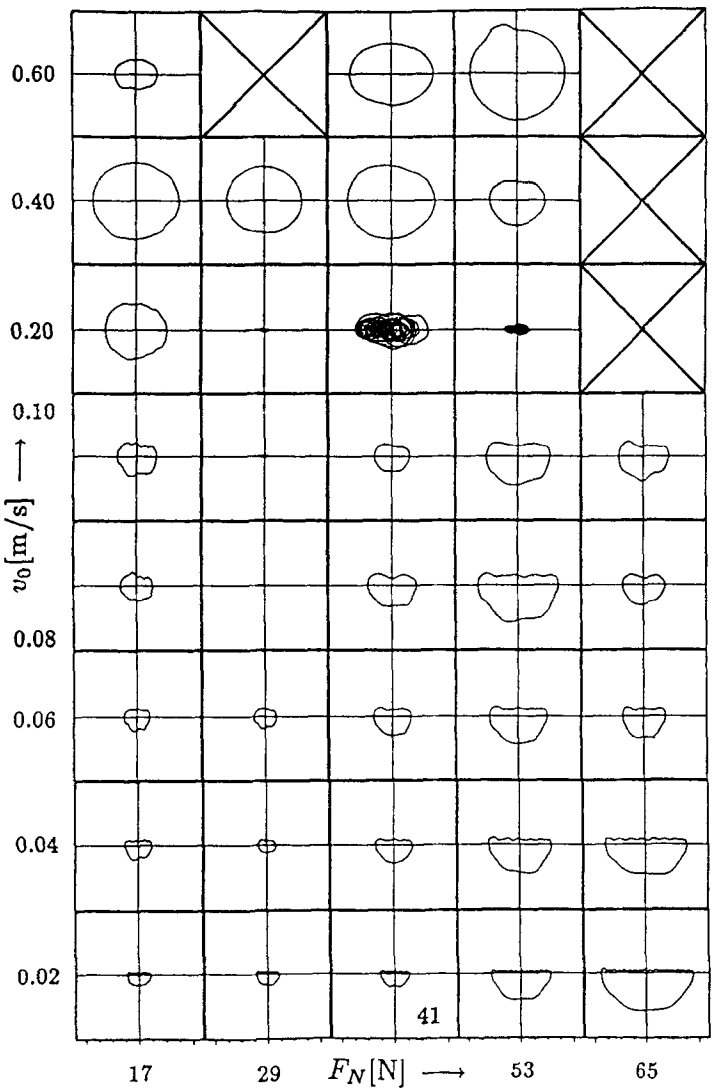

Fig. 9. Measured phase-plane plots of the beam system.

5. Identification of the Friction Characteristic

The direct measurement of the friction characteristic shows that the friction force is influenced by the dynamics of the measuring device itself. In order to obtain the real friction force acting at the contact point during the experiment, an *identification* of the friction force from a measured time series has been carried out, based on equation (3). Following an idea of Mueller [23] we can identify the friction force from a measured time series by means of an extended *state observer*. A linear system equation (9) can be associated with equation (5)

$$\hat{\boldsymbol{x}}' = \hat{\boldsymbol{A}}\hat{\boldsymbol{x}} + \hat{\boldsymbol{b}}F_R(\tau)\,, \tag{9}$$

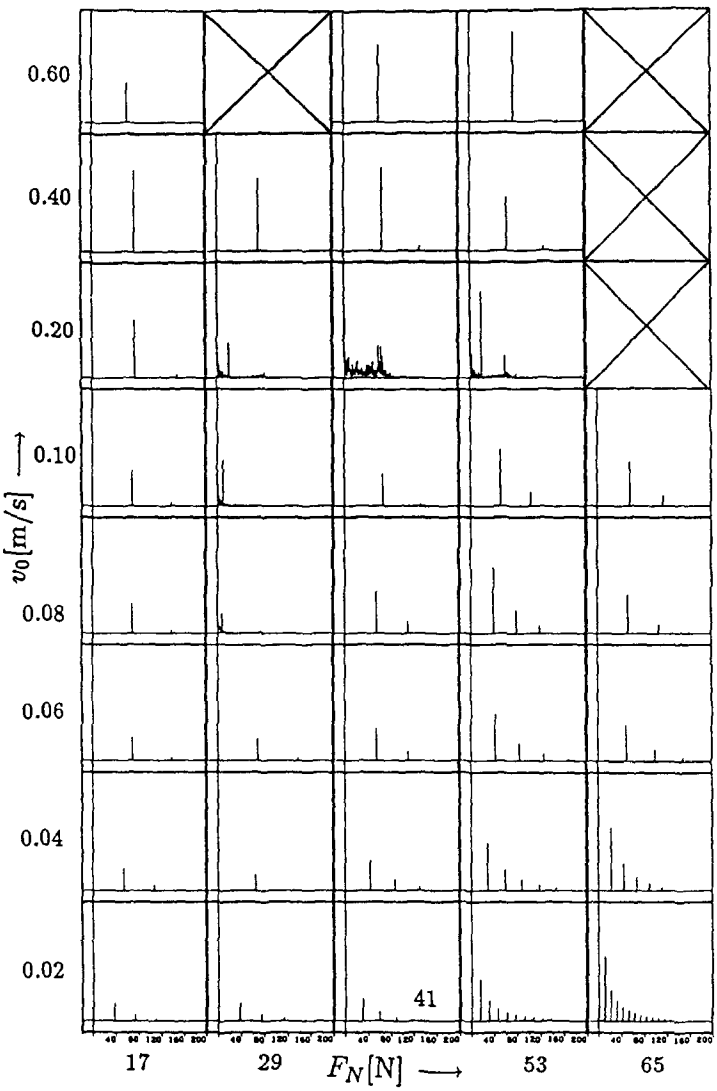

Fig. 10. Fourier amplitude spectra, calculated from the measured data.

with a stepwise constant friction force $F_R(\tau)$, with $F_R'(\tau) = 0$. The block diagram of the state observer is shown in Figure 13. Introduction of an extended state vector $\hat{x}_e^T = [\hat{x}_1, \hat{x}_2, \hat{x}_3, \hat{x}_4, F_R]$, allows the observer of the beam system to be described by the vector equation (10)

$$\hat{x}_e' = \underbrace{[\hat{A}_e - \hat{v}_e \hat{c}_e^T]\hat{x}_e}_{A_B} + \hat{v}_e \tilde{w}(\tau)\,, \quad \hat{x}_e(0) = \hat{x}_{e0}\,, \tag{10}$$

where A_B denotes the extended observer matrix of the beam system,

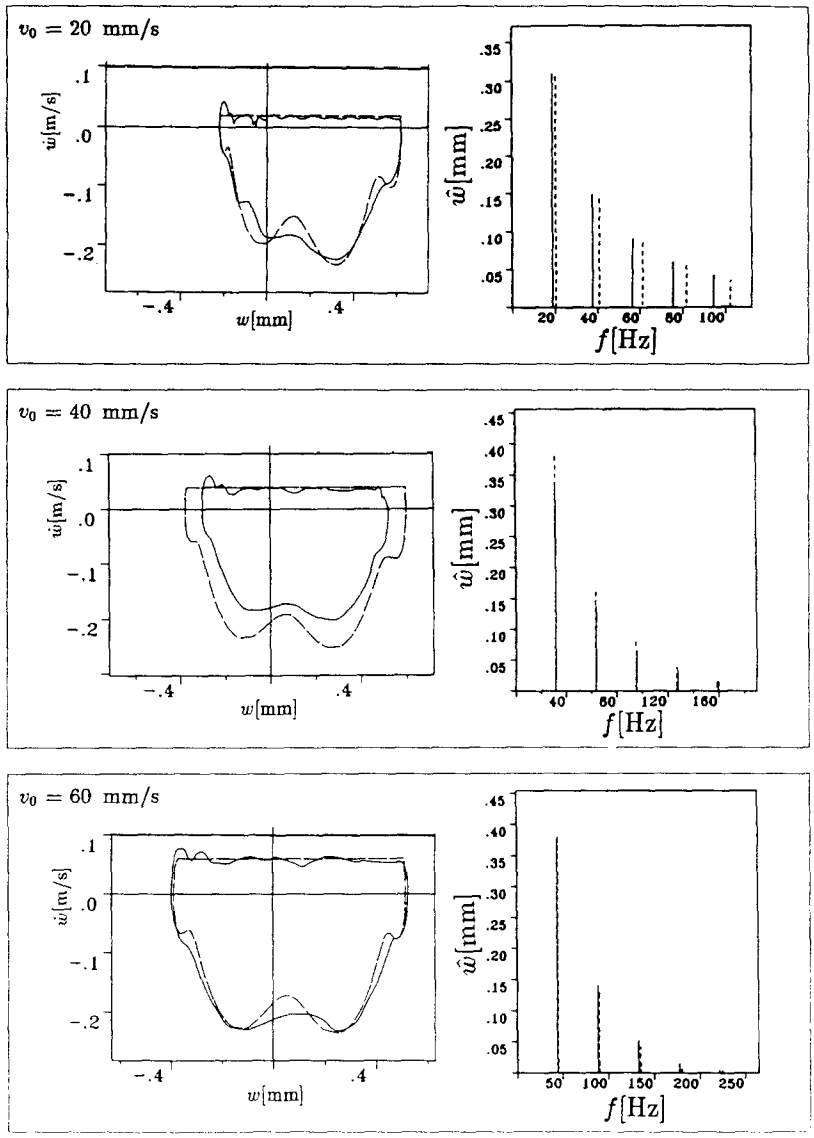

Fig. 11. Comparison between measured and simulated data ($F_N = 36$ N) (—— measured, - - - calculated).

$$\boldsymbol{A}_B = \begin{bmatrix} -\phi_1\hat{v}_1 & 1 & -\phi_2\hat{v}_1 & 0 & 0 \\ -\omega_1^2 - \phi_1\hat{v}_2 & -2D_1\omega_1 & -\phi_2\hat{v}_2 & 0 & b_2 \\ -\phi_1\hat{v}_3 & 0 & -\phi_2\hat{v}_3 & 1 & 0 \\ -\phi_1\hat{v}_4 & 0 & -\omega_2^2 - \phi_2\hat{v}_4 & -2D_2\omega_2 & b_4 \\ -\phi_1\hat{v}_5 & 0 & -\phi_2\hat{v}_5 & 0 & 0 \end{bmatrix}, \tag{11}$$

with the first two eigenfunctions $\phi_{1,2}$ of the beam system, $\hat{\boldsymbol{c}}_e$ is the output vector, $\hat{\boldsymbol{v}}_e$ is the vector which amplifies the error $e = \tilde{w} - \hat{w}$, $\hat{\boldsymbol{x}}_{e0}$ are the initial conditions, and $\tilde{w}(\tau)$ is the measured time series from the beam system. The components of $\hat{\boldsymbol{v}}_e$ have been determined by a pole assignment.

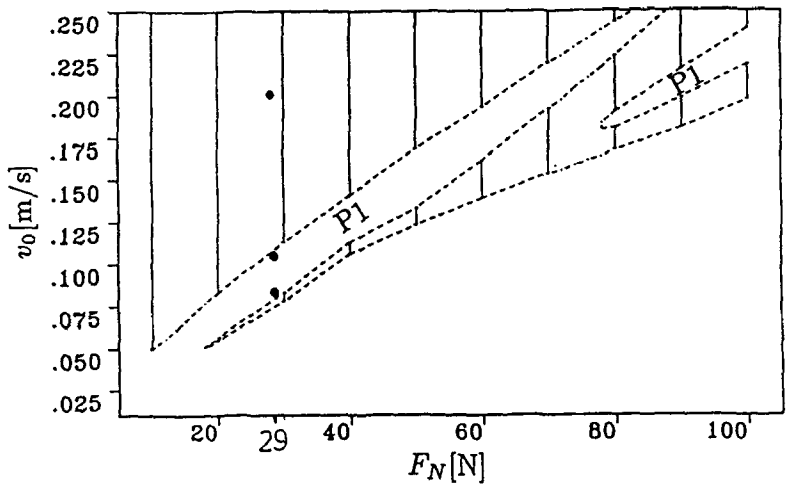

Fig. 12. Part of the F_N, v_0 parameter space with measured data points marked by dots.

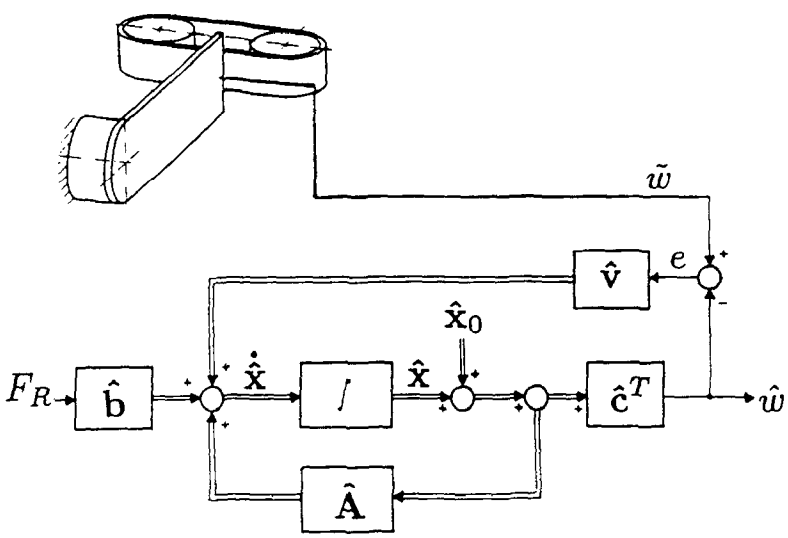

Fig. 13. Block diagram of the modal state observer.

The described state observer allows one to identify the real friction force acting at the contact point, cf. Figure 14. With the relative velocity $v_r = \dot{w}(l) = v_0$, the friction characteristic $\hat{\mu}$ can also be obtained, cf. Figure 14.

6. Characteristic Values of the Time Series

The comparison of measured and calculated data for the beam system show good agreement in the case of a *regular* motion. If one considers a measured *irregular* time series $z(\tau) := \tilde{w}(\tau)$ of the beam system, two questions arise:

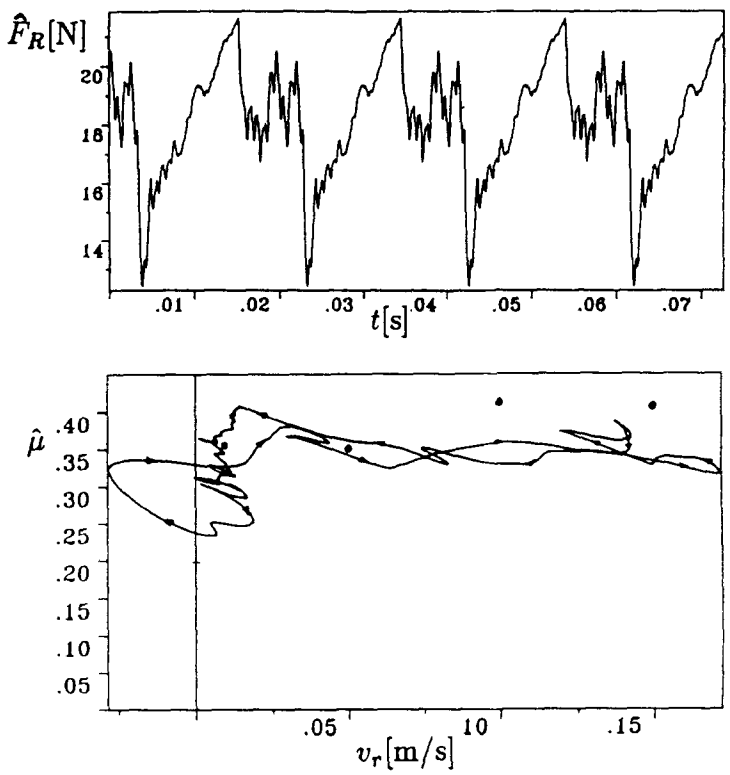

Fig. 14. Identified friction characteristic at the contact point of the beam system. Dots represent measured mean values obtained from the direct measurements.

- Which part of the signal can be described by deterministic equations and which part is noise from the environment?
- How large is the minimum dimension of the state space in which the chaotic attractor can be embedded?

These two questions can be answered by the *correlation integral*, $C(r)$, developed by Grassberger and Procaccia [24]. Before applying the correlation method one has to produce more than one state coordinate, which is possible with a reconstructed *pseudo-state space* due to Packard [25]. The pseudo-state space vectors, z_j, are constructed from the time series with the *time delay method*

$$z_j^T = [w(t_0 + j\,\Delta t) + (k-1)T_S]\,, \quad k = 1(1)m_B\,, \quad j = 1(1)N - \frac{t_0}{\Delta t} - (m_B - 1)\,\frac{T_S}{\Delta t}\,, \tag{12}$$

where T_S denotes the time delay, m_B the embedding dimension, N the number of sampled data points, t_0 is the starting time, and Δt is the time step between two sampled data points. By applying this procedure, *metric* properties, like the shape of the time series, get lost, but the *topologic* properties, like the dimension, will not change, cf. Figure 15. The correlation integral, $C(r)$, can be evaluated from the following equation

$$C(r) = \lim_{N\to\infty} \frac{1}{N} \sum_{j=1}^{N} \frac{1}{N-1} \sum_{\substack{i=1 \\ i\neq j}}^{N} h(r - \|z_i - z_j\|) \tag{13}$$

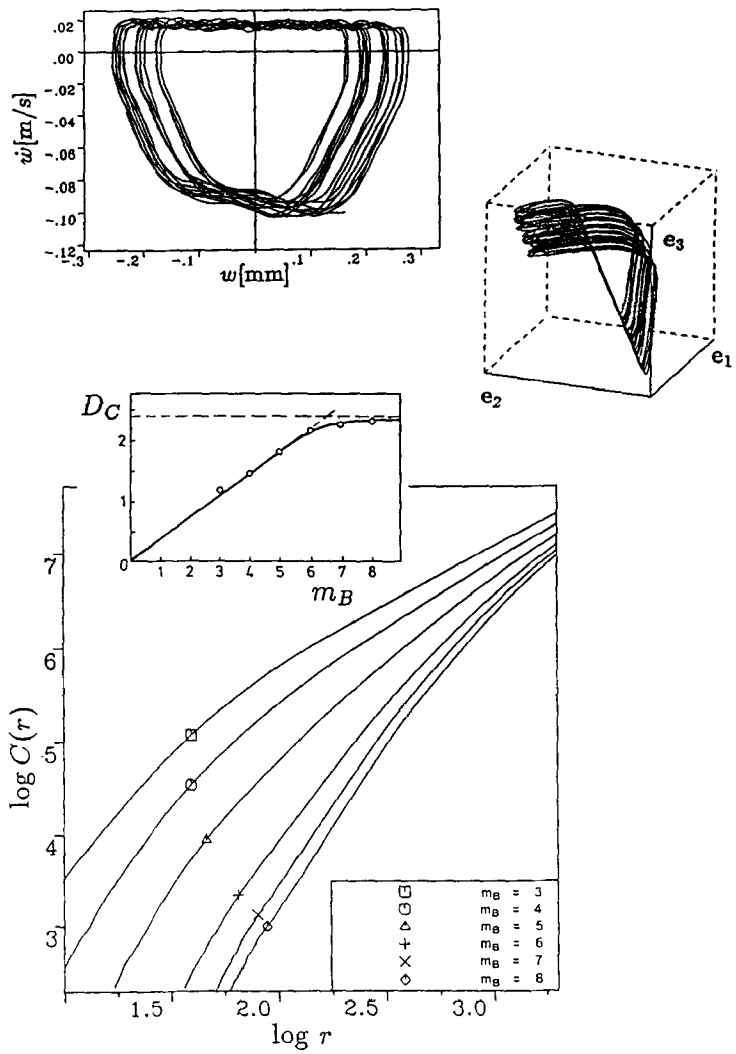

Fig. 15. Embedded *regular* time series and the correlation integral of the beam system with the parameter values $F_N = 41$ N and $v_0 = 20$ mm/s.

where $z_{i,j}$ denotes the measured vectors of the pseudo-state space, h is the Heavyside unit step function, N is the number of sampled points, and r is the radius of a hypersphere.

The value of $C(r)$ is the probability that two points lie within a hypersphere of radius r. It is therefore a measure of the *spatial* correlation of the points in the pseudo-state space. The slope in the median domain of the $C(r)$ diagram on a double logarithmic scale is an estimate of the correlation dimension, D_C, of the chaotic attractor with

$$D_C = \lim_{m_B \to \infty} \frac{\Delta \log C(r, m_B)}{\Delta \log r} . \tag{14}$$

The correlation dimension, D_C, is a lower bound of the fractal dimension, $D_F < D_C$, which gives a measure of the number of the 'active' pairs of state variables of the motion of the attractor, [26].

The calculation of D_C using the correlation integral is more efficient than a direct calculation of D_F using a 'box counting' algorithm. The procedure is straightforward and is based only on re-write and counting operations; i.e., it does not depend on the rate and duration of the signal sampling. Numerical experience shows that the minimum of sampled data has to be about $N = 15\,000$. If one increases the embedding dimension, m_B, the correlation dimension will rise to a constant value. In the case of the beam system $D_C \approx 5.1$ gives a result, cf. Figure 16, which means that, in the chaotic case, more than ten independent state variables are active on the attractor and a description with two modes only, with stationary friction characteristic, is not sufficient to describe the irregular motion. In the regular case a correlation dimension of $D_C = 2.3$ gives a result which means that a four-dimensional state space is quite sufficient to describe the motion. More detailed information concerning these problems is given in [27].

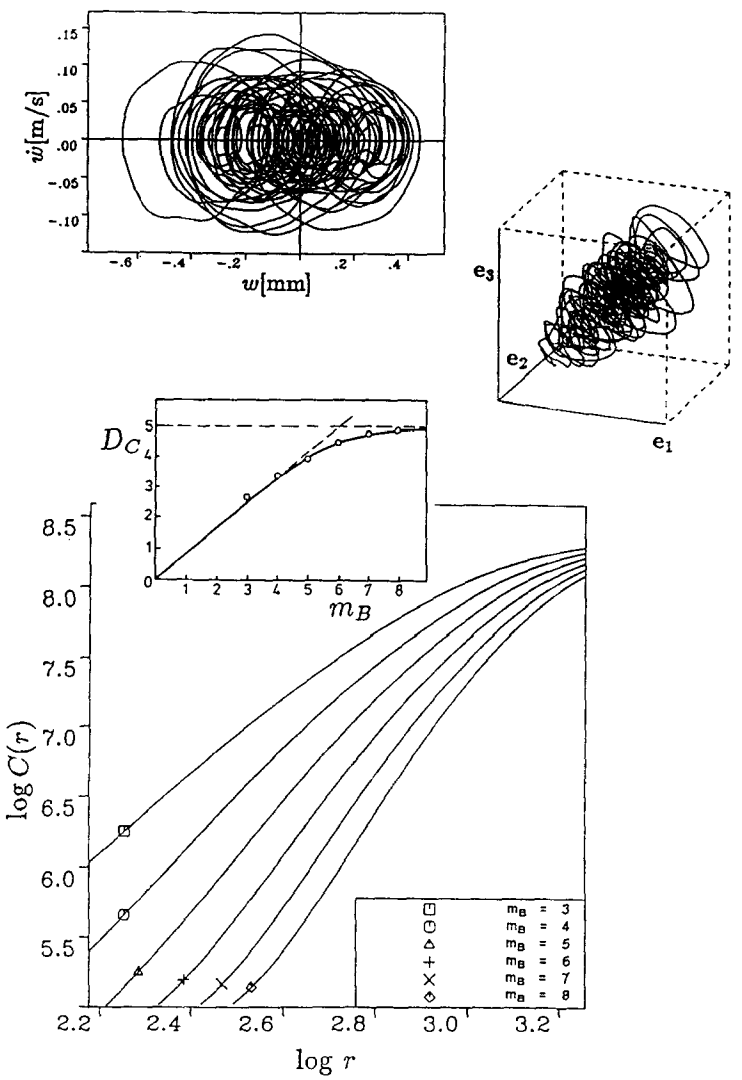

Fig. 16. Embedded *irregular* time series and the correlation integral of the beam system with the parameter values $F_N = 41$ N and $v_0 = 210$ mm/s.

7. Concluding Remarks

Stick-slip vibrations are friction-induced, self-sustained oscillations. They occur in many engineering systems as well as in everyday life. In the case of a continuous beam system, the limit cycle behavior, obtained numerically, has been compared with measured data. It turned out to that the regular motion can be well described by a model with two bending mode shapes and a stationary friction characteristic.

If a system comprises a linear part and nonlinearities it is easier to identify the nonlinearities from a measured time series by means of a modal state observer, rather than to measure it in a separate experiment.

The behaviour of the correlation integral has allowed us to obtain the correlation dimension for a chaotic motion of the beam system. This scalar quantity gives an estimate of the dimension of the attractor, and it thus contains information about the order of the system, required in an adequate mathematical model. But in practice it is only a hint for the *minimum* number of state coordinates. It does not tell the engineer how large a number of mode shapes has to be taken into account, in the case of a continuous system.

Acknowledgements

This research has been performed at the University of Hannover, Germany, under the supervision of Prof. Dr.-Ing. K. Popp and has been financed by the Volkswagen foundation under the contract No. I/63177. I acknowledge this support with gratitude and I would also like to thank former students Thomas Pfingsten, Thorsten Schade, Wolfgang Schleef, Andreas Harms, Stefan Viola, Hermann Herbers and Hans G. Jacob who have contributed to this research by their project work.

References

1. Moon, F. C. and Shaw, S. W., 'Chaotic vibrations of a beam with non-linear boundary conditions', *International Journal of Non-Linear Mechanics* **18**, 1983, 465–477.
2. Hendriks, F., 'Bounce and chaotic motion in impact print hammers', *IBM Journal of Research and Development* **27**, 1983, 24–31.
3. Springer, H. and Ullrich, M., 'Dynamics of dot-matrix printers', *Proceedings of IUTAM Symposium on Nonlinear Dynamics in Engineering Systems*, University of Stuttgart, FRG, Aug. 21–25, 1990, Springer, Berlin, 297–304.
4. Szczygielski, W. M., 'Dynamisches Verhalten eines schnell drehenden Rotors bei Anstreifvorgängen', Zürich, ETH, Dissertation , No 8094, 1986.
5. Kaas-Petersen, Chr. and True, H., 'Periodic, biperiodic and chaotic dynamical behavior of railway vehicles', *Proceedings 9th IAVSD-Symposium*, Linkoping, 1985, 208–221.
6. Grabec, I., 'Explanation of random vibrations in cutting on grounds of deterministic chaos', *Robotics & Computer-Integrated Manufacturing* **4**, 1988, 129–134.
7. Pfeiffer, E., 'Seltsame Attraktoren in Zahnradgetrieben', *Ingenieur-Archiv* **58**, 1988.
8. Magnus, K., *Schwingungen*, Teubner, Stuttgart, 1961.
9. Marui, E. and Kato, S., 'Forced vibration of a base-exited single-degree-of-freedom system with Coulomb friction', *Transaction ASME, Journal of Dynamical Systems, Measurement and Control* **106**, 1984, 280–285.
10. Miyamoto, M., 'Effect of dry friction in link suspension on forced vibration of two-axle car', *Quarterly Reports* **14**, 1973, 99–103.
11. Den Hartog, J. P., 'Forced vibrations with continued Coulomb and viscous friction', *Transaction ASME APM-53* **9**, 1931, 107–115.

12. Popp, K. and Stelter, P., 'Stick-up vibrations and chaos', *Philosophical Transactions of the Royal Society, London* **A332**, 1990, 89–105.
13. Utkin, V. I., *Sliding Modes and Their Application in Variable Structure Systems*, English Translation Moscow: MIR Publication, 1978.
14. Pratt, T. K. and Williams, R., 'Non-linear analysis of stick/slip motion', *Journal of Sound and Vibration* **74**, 1981, 531–542.
15. Dowell, E. H. and Schwartz, H. B., 'Forced response of an cantilever beam with a dry friction damper attached. I. Theory', *Journal of Sound and Vibration* **91**, 1983, 255–267.
16. Ferri, A. A. and Dowell, E. H., 'The behavior of a linear, damped modal system with a non-linear spring-mass – dry friction damper system attached. II', *Journal of Sound and Vibration* **101**, 1985, 55–74.
17. Shaw, S. W., 'Forced vibrations of a beam with one-sided amplitude constraint: theory and experiment', *Journal of Sound and Vibration* **99**, 1985, 199–212.
18. Popp, K. and Stelter, P., 'Nonlinear oscillations of structures induced by dry friction', *Proceedings of IUTAM Symposium on Nonlinear Dynamics in Engineering Systems*, University of Stuttgart, FRG, Aug. 21–25, 1990, Springer, Berlin, 233–240.
19. Stelter, P. and Popp, K., 'Chaotic behaviour of structures excited by dry friction forces', *Proceedings of Workshop on Rolling Noise Generation, Berlin* (ed. M. Heckl), 1989, 102–111.
20. Stelter, P., 'Reibungserregte Schwingungen eines Kragbalkens', *ZAMM 71*, 1991, 75–78.
21. Stelter, P., 'Nichtlineare Schwingungen reibungserregter Strukturen', *VDI Fortschrittsberichte, Reihe 11 Schwingungstechnik* **137**, 1990.
22. Stelter, P. and Sextro, W., 'Bifurcations in dynamical systems with dry friction', *Proceedings of Bifurcations and Chaos*, Wurzburg, Aug. 20–24, 1990, Birkhauser, Basel, 311–315.
23. Mueller, P. C., 'Indirect measurement of nonlinear effects by state observers', *Proceedings of IUTAM Symposium on Nonlinear Dynamics in Engineering Systems*, University of Stuttgart, FRG, Aug. 21–25, 1990, Springer, Berlin, 205–215.
24. Grassberger, P. and Procaccia, I., 'Measuring the strangeness of strange attractors', *Physica* **9D**, 1983, 189–208.
25. Packard, N. H., Crutchfield, J. P., Farmer, J. D., and Shaw, R. S., 'Geometry of time series', *Physical Review Letters* **45**, 1980, 712–716.
26. Leven, R. W., Koch, B.-P., and Pompe, B., *Chaos in dissipativen Systemen*, Akademie-Verlag, Berlin, 1989.
27. Stelter, P. and Pfingsten, T., 'Calculation of the fractal dimension via the correlation integral', *Chaos, Solitons and Fractals – Applications in Science and Engineering*, Pergamon Press, New York, 1991.